2.3 Discussion

Many investigations have been carried out to explore the electron-transfer mechanism in the mitochondrial steroid hydroxylase system of the adrenal cortex which, however, still remains unclear. In this thesis an alternative approach, which is based on a light-induced AR-free reduction of bovine adrenodoxin, was used in order to probe the "shuttle" model for the electron transfer. For this purpose Adx(1-108) was covalently modified with the ruthenium bipyridyl complex.

The results reveal three important findings which concern: (i) the successful labeling of Adx with the ruthenium complex and analysis of its 3D structure, (ii) the kinetics of the light-induced reduction of the iron-sulfur cluster of Adx *via* the labeled ruthenium(II) bipyridyl complex; and (iii) the number of transferred electrons per mole of Adx and its significance for the electron-transfer mechanism.

2.3.1 $Ru(bpy)_2(mbpy)$-Adx(1-108) complex

Background for the use of recombinant His-tagged Adx in the present investigation. During purification from adrenal glands, native bovine Adx is susceptible to proteolysis, resulting in C-terminal heterogeneity [Hiwatashi et al., 1986]. Thus, the amino acid sequence of Adx determined by protein sequencing [Tanaka et al., 1973] is 14 amino-acid residues shorter from the C-terminus than that deduced from the cDNA sequence [Okamura et al., 1985]. This COOH-terminal segment is an integral part of Adx, and its cleavage is not an example of COOH-terminal processing of a nuclear-coded protein destined for mitochondria [Bhasker et al., 1987]. Proteolysis of native Adx during purification may be the result of contamination of adrenal cortex preparations with small amounts of adrenal medulla containing trypsin-like and carboxypeptidase activities [Cupp & Vickery, 1989]. Because homogeneous preparations of a protein are critical, e.g. for crystallization, it is often advantageous to rely on recombinant proteins. They may be easily and reproducibly purified from *E. coli* in the desired quantities.

In laboratory scale purification strategies, ASP is still often used as the first purification and concentrating procedure even for recombinant proteins. Sometimes, the precipitation reaction with $AmSO_4$ should be performed at low temperatures to prevent protein denaturation. The ammonium sulfate must be added slowly, and mixing is important to distribute $AmSO_4$, and

to prevent inclusion of unwanted proteins in the precipitate. This procedure may be time-consuming. However, it was used in the initial purification of Adx(WT), AR, and $P450_{scc}$, since none of the recombinant proteins carried any affinity tag and $P450_{scc}$ was even purified as a native protein from the mitochondria of the adrenal cortex.

The advantage of using an IMAC as the first purification step for the His-tagged proteins is in its simplicity and speed compared to ASP. The IMAC technique can also help to concentrate a protein during purification, so that a higher yield may be obtained. While certain affinity tags might be beneficial to the crystallization of certain proteins, affinity tags are generally believed to be either neutral or detrimental to the crystallization experiment [Bucher et al., 2002]. An alternative to the crystallization of proteins carrying tags is to either dispense with the tag or to use specific proteases to remove them.

In the purification of Adx(N-6×His tag/Xa/1-108), IMAC was used instead of ASP. Factor Xa was chosen as a cleavage enzyme for removing of the tag, because of the high specificity of this protease: It recognizes only a sequence of four amino-acid residues, IEGR [Nagai et al., 1985], and it cleaves the peptide bond between the Gly and Arg residues. Thus, the 6×His tag of Adx(1-108) and the cleavage site was completely removed. The Adx(1-108):Xa ratio of 10:1 was experimentally found to be optimal in order to achieve the highest protease specificity and to decrease unwanted proteolysis at secondary sites. Mass spectrometry data can be taken as proof of the correct choice of conditions for the cleavage reaction (Figure 2.2.6.1.A). Adx(1-108) was further used for covalent modification with $Ru(bpy)_2(mbpy)$.

$Ru(bpy)_2(mbpy)$-modified Adx(1-108) and its properties. In 1988, *Cupp* and *Vickery* [Cupp & Vickery, 1988] wrote regarding the free Cys95 of bovine adrenodoxin: "Whereas cysteine 95 of adrenodoxin is not required for coordination of the iron-sulfur cluster or electron transport with cytochrome *c*, adrenodoxin reductase, or cytochromes $P450_{scc}$, and P45011β, it is conserved among the ferredoxins from the four vertebrate sources sequenced so far. It is therefore possible that the thiol may serve some other, as yet unknown, function." In this doctoral thesis, this cysteine served as a specific modification site for binding of the ruthenium complex to study the mechanism of electron transfer.

Adx(1-108) was labeled with $Ru(bpy)_2(mbpy)$[21] to obtain a specific complex of 1:1 ratio between the two components. This stoichiometry of the complex was necessary for the subsequent investigation. However, the spectral- and SDS-PAGE-analysis revealed the presence

[21] The mechanism of modification reaction is described in the Methods section.

of samples with different complex-to-Adx(1-108) ratios, in the range of 0.6-1.2, after purification of a crude mixture on an anion-exchange chromatography column (Figure 2.2.5.1.B). This might be due to the presence of several potential modification sites. Other sites could be lysine and histidine residues, as described in section 1.3.2. Bovine adrenodoxin has five lysine residues at positions 6, 22, 24, 66 and 98, and three histidine residues at positions 10, 56 and 62. Nevertheless, the fraction of the specific Cys95-modified (50-60% of total amount of Adx(1-108) used for coupling[22]) adrenodoxin was of primary interest. Unspecific labeling was shown to take place when the Adx mutant with a Cys95-to-Ser95 substitution was coupled with the ruthenium(II) bipyridyl complex. However, for this mutant, no specific 1:1 complex could be purified, which may be taken as proof that Cys95 is the main site of covalent modification site for Adx(1-108). ES-TOF-MS data confirmed the formation of 1:1 $Ru(bpy)_2(mbpy)$-Adx(1-108) complex[23] (Figure 2.2.6.1.B).

After successful modification, bovine Adx(1-108) was characterized by different methods to find out if the labeling has any effect on the protein function. It is known that the ability to accept and donate electrons is tightly connected to the redox potentials of the iron-sulfur cluster of ferredoxin proteins [Uhlmann & Bernhardt, 1995]. The water accessibility of the prosthetic group, charge distribution, overall protein dipole, and hydrogen-bonding network around the cluster affect the redox potential [Uhlmann & Bernhardt, 1995; Grinberg & Bernhardt, 2001; and Beckert & Bernhardt, 1997]. The bound ruthenium complex protrudes from the protein surface and is oriented toward the [2Fe-2S] cluster (Figure 2.2.9.6.A). This position of the complex might affect the cluster microenvironment and, as a consequence, its midpoint potential. However, the measured redox potentials of $Ru(bpy)_2(mbpy)$-Adx(1-108) (–306 mV) and Adx(1-108) (–302 mV) are almost identical, indicating an intact iron-sulfur cluster environment. However, differences in the kinetics of cytochrome *c* reduction between $Ru(bpy)_2(mbpy)$-Adx(1-108) and Adx(1-108) have been observed, suggesting that labeling may affect intermolecular electron transfer (Table 2.2.8.1). The slowest kinetics observed in the cytochrome *c* reduction with $Ru(bpy)_2(mbpy)$-Adx(1-108), in spite of its identical redox potential with the unmodified Adx(1-108), can be explained by steric hindrance when $Ru(bpy)_2(mbpy)$-Adx(1-108) and the cytochrome interact (Figure 2.2.8.1.C).

[22] 5-10% of the total Adx used in the modification reaction were expected to be degraded due to the presence of DMSO.

[23] Further conformation of the modification site was obtained after the crystal structure of the $Ru(bpy)_2(mbpy)$-Adx(1-108) complex was solved.

Further, studies of the functionality of the $Ru(bpy)_2(mbpy)$-Adx(1-108) in NADPH-induced reduction of $P450_{scc}$ showed that this Adx is able to shuttle the electrons from AR to the side-chain cleavage cytochrome in the reconstituted steroid hydroxylase system (Figure 2.2.8.1.A). Moreover, no significant differences in the spectral changes during the reaction were observed when one of three adrenodoxins, Adx(WT), Adx(1-108), and $Ru(bpy)_2(mbpy)$-Adx(1-108), was used as electron carrier. However, it is not excluded that modified Adx(1-108) may also affect the protein-protein interaction with both AR and $P450_{scc}$.

Based on the known crystal structure of the cross-linked complex between AR and Adx [Müller, J. J. et al., 2001] and cross-linking studies between Adx and $P450_{scc}$ [Chu & Kimura, 1973], it was concluded that the acidic region of the interaction domain (residues 72-79) of Adx is important for binding of the ferredoxin to its redox partners. Thus, a similar geometry of protein-protein interactions, and hence, a similar orientation of Cys95 of Adx relatively to the protein matrix of AR and $P450_{scc}$ is expected. Indeed, for the AR-Adx complex structure the detailed geometry of the protein-protein interactions was described [Müller, J. J. et al., 2001]. In this structure, Cys95 of Adx is tilted toward the protein-protein interaction surface, i.e. toward the AR matrix. The ruthenium moiety of $Ru(bpy)_2(mbpy)$ covalently bound to Adx at Cys95, will therefore be also oriented toward the reductase (Figure 2.3.1.1.A and Figure 2.3.1.1.B). Assuming geometry of the cross-linked AR-Adx complex, in possible complex between ruthenated Adx(1-108) and AR, the covalently attached ruthenium complex would be relatively far away from the surface of AR (Figure 2.3.1.1.A). In the $Ru(bpy)_2(mbpy)$-Adx(1-108)-$P450_{scc}$ complex, shown in Figures 2.3.1.1.C and 2.3.1.1.D, the ruthenium(II) bipyridyl complex will be in the close vicinity of the cytochrome surface. Whereas the ruthenium moiety does not perturb the reductase matrix (Figure 2.3.1.1.A), as it does for the complex of modified Adx(1-108) with cytochrome *c*[24] (Figures 2.3.1.1.E and 2.3.1.1.F), it may slightly disturb the docking of the coupled Adx on $P450_{scc}$ (Figure 2.3.1.1.C). Since the theoretical model (PDB ID 1scc) of $P450_{scc}$ was used in modeling of Adx-$P450_{scc}$ complex, there could be some inaccuracy in the modeling.

[24] The $Ru(bpy)_2(mbpy)$-Adx(1-108)-cytochrome *c* complex is shown so that if the uncoupled Adx would interact with the cytochrome. But, this indicates that such $Ru(bpy)_2(mbpy)$-Adx(1-108)-cytochrome *c* complex is impossible, since the ruthenium moiety perturbs the heme-protein surface. On the other hand, it suggests that if modified Adx(1-108) would interact with the cytochrome *c*, the geometry of the complex will be different from that of unmodified ferredoxin with the cytochrome. The same is true for the complex with $P450_{scc}$.

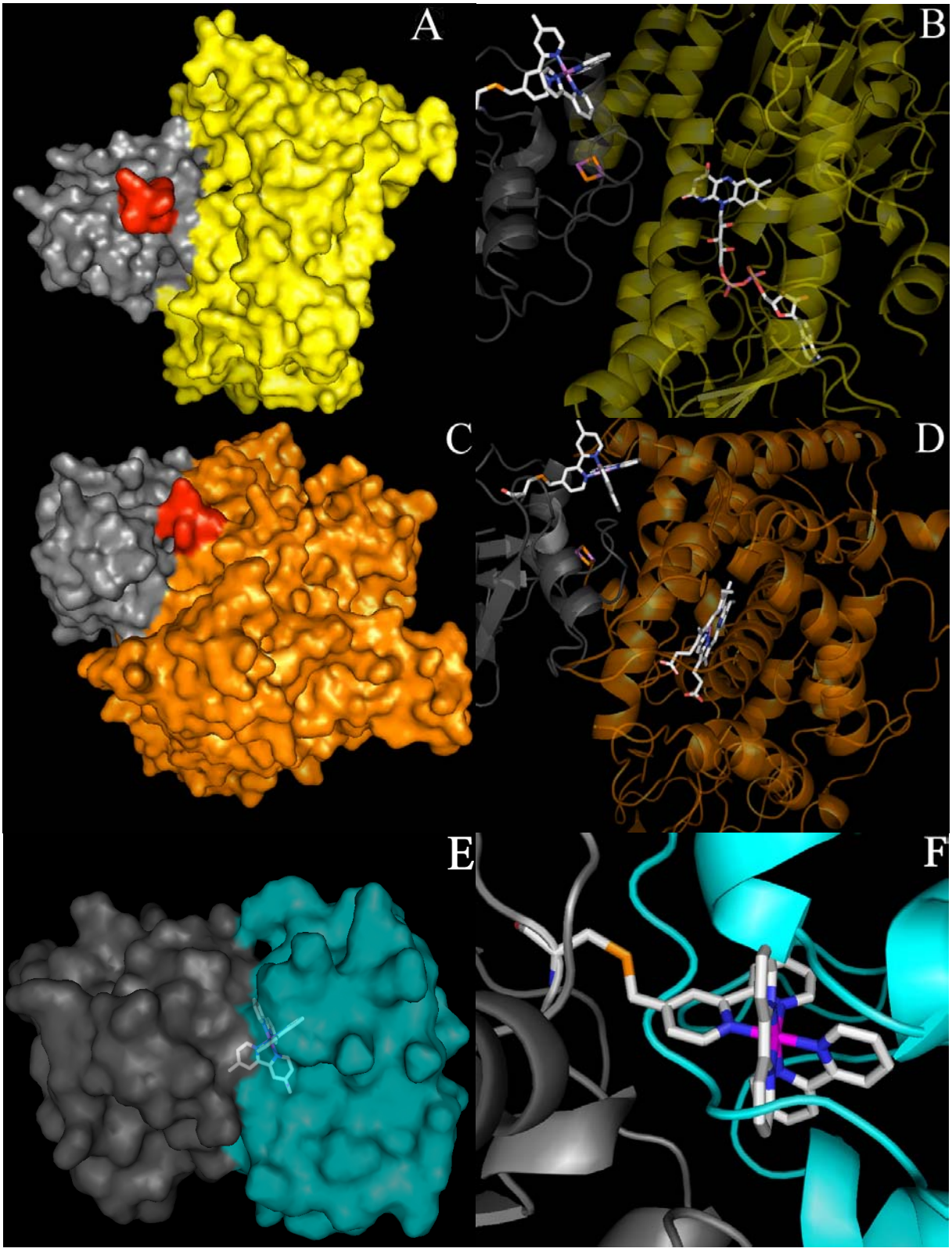

Figure 2.3.1.1 Protein-protein interaction between $Ru(bpy)_2(mbpy)$-Adx(1-108) and its redox partners. A, C, E. Surface representations of the $Ru(bpy)_2(mbpy)$-Adx(1-108)-AR, $Ru(bpy)_2(mbpy)$-Adx(1-108)-$P450_{scc}$, and $Ru(bpy)_2(mbpy)$-Adx(1-108)-cytochrome *c* complexes. Adx(1-108) in grey, AR in yellow, $P450_{scc}$ in orange, cytochrome *c* in cyan, Δ-isomer of the ruthenium complex in red (in complexes with AR and $P450_{scc}$) and in sticks

representation in case of the complex with cytochrome *c*. B, D, F. Cartoon views of the complexes. Redox groups of Adx, AR, and $P540_{scc}$ are drawn in sticks. The ruthenium complex (in sticks) is covalently bound to Cys95, shown in sticks representation, too. Ruthenated Adx(1-108) was fitted in the complexes of unmodified Adx with its redox partners using LSQKAB [Kabsch 1976]. Pictures were generated by the program PyMOL (DeLano Scientific LLC, USA).

However, from such a modeling of unmodified Adx with cytochrome *c* and $P450_{scc}$, as well as the crystal structure of the cross-linked AR-Adx complex, it cannot be concluded with confidence that the modified Adx(1-108) will or will not change the mode of protein-protein interaction.

Crystal structure of the Ru(bpy)$_2$(mbpy)-Adx(1-108) complex. Crystallization of the covalent 1:1 Ru(bpy)$_2$(mbpy)-Adx(1-108) complex and its structure analysis were necessary to identify the modification site and to predict intramolecular electron-transfer pathways within the complex. This is the first crystal structure of bovine adrenodoxin in the complex with a transition ruthenium(II) bipyridyl complex. It is also the best resolved structure of bovine Adx so far.

The presence of two isomer of the ruthenium complex complicated the refinement of the structure. Since the electron density of some of the bipyridyl ligands of the compound was not well resolved (Figure 2.2.9.2.C), it was difficult to find the proper orientation of both isomers that would decrease the *R*-factors during refinement. Nevertheless, the density of the bipyridyl ligand, which makes the covalent link with Cys95 of Adx, was quite well resolved and, therefore, was used as a start point in the density improvement using the program EDEN (Figures 2.2.9.3.A and 2.2.9.3.B). The EDEN-generated density, carrying the properties of an omit map, showed clearer contours for the ruthenium complex. This helped to correctly orient both isomers within the omit map and to refine new positions of the isomers. Moreover, this method of electron density generation provided an indication how the side chains of Cys95 should be refined according to the presence of the compound isomers (Figures 2.2.9.3.C and 2.2.9.3.D).

The presence of two Ru(bpy)$_2$(mbpy) isomers in the crystal structure had no influence on the overall protein fold. A validation of the structure with PROCHECK [Laskowski et al., 1993; Morris et al., 1992] revealed a good stereochemical quality of the structure (Figure 2.2.9.4). There were no forbidden amino-acid conformations in the vicinity of the ruthenium complex, indicating that the coupled ruthenium(II) bipyridyl complex has no influence on the nearby protein structure. This is in agreement with the very similar redox potentials determined for Adx(1-108) and Ru(bpy)$_2$(mbpy)-Adx(1-108). Additionally, a comparison of the oxidized

Adx(4-108) [Müller et al., 1998] and full-length reduced structures [Beilke et al., 2002], solved by X-ray crystallography and NMR, respectively, with the structure of $Ru(bpy)_2$(mbpy)-Adx(1-108), did not revealed any differences in the folding of the core domain and most of the interaction domain (Figure 2.2.9.5). Only the interaction F-helix of the latter domain in the NMR structure is moved away from its position in oxidized adrenodoxin [Beilke et al., 2002]. Since the ruthenium complex is tilted more toward the [2Fe-2S] cluster of the protein than in any other directions, e.g. toward the F-helix, after reduction of the $Ru(bpy)_2$(mbpy)-Adx(1-108) complex the rearrangement of the interaction domain, and hence, protein-protein interaction with the redox partners would be possible. However, as it was already discussed above, during protein-protein interaction of the $Ru(bpy)_2$(mbpy)-Adx(1-108) with its redox partners, the complex might change the interaction geometry between redox partners. Indeed, this will also change the distances between the redox groups of proteins, and hence, the rate of electron transfer, i.e. the kinetics of the oxidation-reduction reactions. This is in a good agreement with the theoretical data (section 1.2) pointing out that the rate of electron transfer will decrease with increasing of the distance between two reactive centers and *vice versa*.

2.3.2 Kinetics of the light-induced reduction of the iron-sulfur cluster of Adx

Photoexcitable dyes such as safranin T, lumiflavine [Hintz & Peterson, 1980], proflavine, acridine [Tyson et al., 1972], or Brilliant Alizarin Blue [Sligar & Gunsalus, 1976] have been utilized for a long time to reduce ferric $P450_{cam}$ and other proteins in connection with a sacrificial electron donor like EDTA. A new strategy for the design of various dyes, consisting of a heme-unit bridged with the photo-active molecule $Ru(bpy)_3$ was recently developed. The main advantage of such chemically ruthenium-modified proteins is that protein may be reduced by flash photolysis without participation of proteins partners in an electron transfer. Ruthenium complex labeling of different heme proteins such as cytochrome b_5 and cytochrome *c* has originally been established by several laboratories to study intramolecular electron-transfer routes and to check the different distance dependence models of transfer [Scott et al., 1993; Sun et al., 1995].

It is implicitly assumed that only the intramolecular electron transfer is significant. However, the present studies show that the electron-transfer rate depends on the concentration of the ruthenium-labeled Adx(1-108), indicating intermolecular transfer taking place (k_{et2} = ~8×10^6

M^{-1} s^{-1}). The intermolecular electron transfer was also observed in previous studies of ruthenium complex-labeled cytochrome $P450_{cam}$ [Contzen et al., 2002]. Extrapolation to zero Adx concentration gives the intramolecular rate constant, which is found to be ~81 s^{-1}. Considering the driving force ΔG of ~0.5 V for the excited state of the ruthenium complex ($Ru(II)^*$) to oxidized Adx(1-108) estimated from the redox potentials of ~ –0.8 V [Juris et al., 1988] and ~ –0.3 V for the $Ru(II)^*$ and the [2Fe-2S]-cluster, respectively, the distances of ~7-9 Å has been determined from the Dutton plot. This distance range is close to the average edge-to-edge distances of 9-10 Å from the ruthenium ligand (C^{23} or C^{21} atom) to Fe2 of the iron-sulfur cluster in Adx (Figure 2.2.9.6.B), but it is smaller than those that were computed using the program HARLEM.

Whereas Δ-$Ru(bpy)_2(mbpy)$ in both chains (Figures 2.3.2.1.A and 2.3.2.1.C) occupy approximately the same position relatively to Cys92, as the electron acceptor in the pathways *via* that residue, the edge-to-edge distance between the C^{21} atom of the Λ-isomer in molecule B and the Fe2 atom is increased by ~1-1.5 Å (Figures 2.3.2.1.B and 2.3.2.1.D). This may be the reason for the presence of an alternative predicted intramolecular path in this isomer. In molecule B, a 24-Å pathway from the Λ-isomer (Figure 2.2.9.6) *via* the backbone (residues 95, 94, 93, and 92) of the protein to Fe2 is more likely according to the comparative calculation of all possible coupling decay factors performed by HARLEM (see section 1.2.4.1). Namely, the through-space coupling factors calculated by HARLEM suggest that the through-space jump to Cys92 is to be more favorable from the C^{21} of Λ-$Ru(bpy)_2(mbpy)$ in chain A, only. Indeed, the edge-to-edge distances between the C^{21} atom of the MLCT state of the ruthenium complex and the O atom of Cys92 are ~4 Å and ~5 Å in chains A and B, respectively. Thus, the increased distance (5 Å) will not favor the tunneling *via* through-space, because the energy barrier will be then higher, than it is allowed for those jumps, i.e. the pathway will occur *via* the covalent bonds of Cys95, Ile94, Gln93, and Cys92, where the barrier is generally lower [Onuchic et al., 1992].

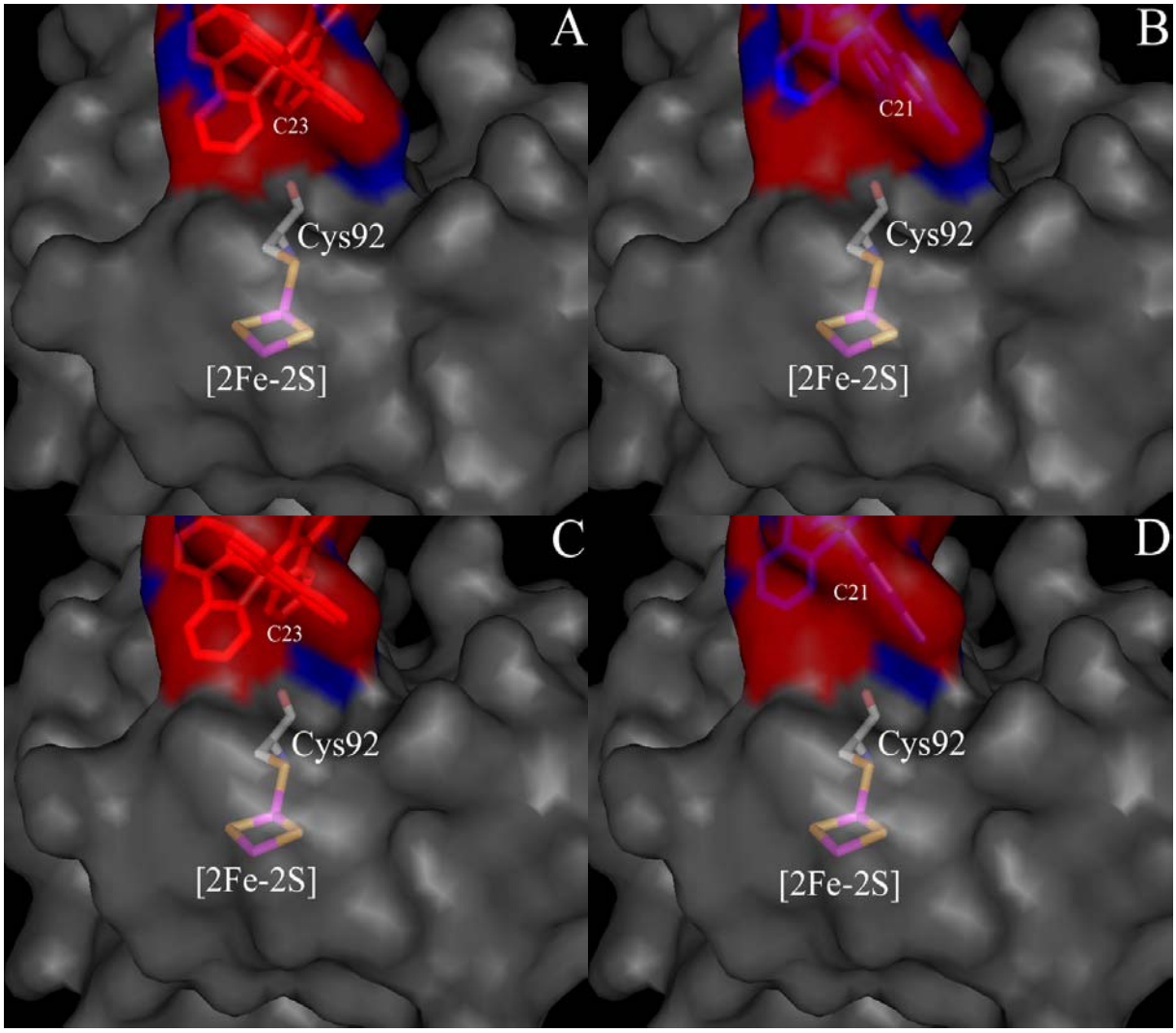

Figure 2.3.2.1 Position of the $Ru(bpy)_2(mbpy)$-isomers within the $Ru(bpy)_2(mbpy)$-Adx(1-108) complex (top view of the Figure 2.2.9.6.A). A. and B. Chain A with Δ- (red) and Λ-isomer (blue) of the ruthenium complex, respectively. C. and D. Chain B with Δ- (red) and Λ-isomer (blue) of the ruthenium complex, respectively. In all pictures the [2Fe-2S] cluster of Adx(1-108) (grey) is drawn in sticks representation with iron atoms in magenta and sulfurs in yellow. Also, Cys92, as a terminal residue, which accepts an electron from the MLCT state of the ruthenium(II) bipyridyl complex, is shown in sticks view. The C^{23} and C^{21} atoms of the MLCT states are shown (for more details see Figure 2.2.9.6). Pictures were generated by the program PyMOL.

According to the concept of the Dutton plot [Page et al., 1999], the electron-transfer rate is determined only by the distance between the redox pair (e.g. in the present work 7-9 Å), with specific electron tunneling pathways being insignificant in biological electron transfer. This is a big difference from the "pathway" [Onuchic et al., 1992] model in which specific tunneling paths (e.g. in this manuscript 12-13 Å) are expected to play a more significant role in biological electron transfer. The obtained distances/paths can not be compared, in spite of small difference

between them, because the theoretical background for their determination is different. Nevertheless, if one assumes recently developed [Kawatsu et al., 2000; Kawatsu et al., 2001] a novel "worm" model for determining the electron-transfer pathways, one can reconcile the “straight-line” and “pathway” models. The "worm" is more or less a straight line but, on the other hand, it winds, reflecting the specific role of the microenvironment of the protein structure. Thus, based on this assumption the present HARLEM-determined pathways (~12-13 Å) and Dutton distances (~7-9 Å) are: (i) in the distance range for biological electron transfer [Page et al., 1999]; and (ii) could be interpreted to the calculated intramolecular rate constant.

Nevertheless, from the above discussion, the position of two configurations of the ruthenium complex, and in particular Λ-$Ru(bpy)_2(mbpy)$, is a question of more refinement, and hence, a question of a preferential electron-transfer pathway, which then can be calculated using the crystal structure coordinates. On the other hand, the difference of 1 Å between the positions of the C^{21} atoms of two Λ-$Ru(bpy)_2(mbpy)$ that leads to the alternative 24-Å pathway, may also be biologically relevant. It does, however, not correspond to the experimentally determined intramolecular monomolecular rate. Nevertheless, such big distances, when determined as direct donor-acceptor distances, were shown by the “worm” model [Kawatsu et al., 2000; Kawatsu et al., 2001] to be supported for electron tunneling *via* the through-space and through-bond routes. It is not also excluded the possibility that electronic coupling through solvent molecules can compete with covalent-bridge- and through-space-mediated coupling. The role of water as a medium for electron transfer has been investigated [Marcus & Sutin, 1985].

To summarize, the 3D structure of the $Ru(bpy)_2(mbpy)$-Adx(1-108) complex determined at 1.5 Å resolution provides suggestions of distinct electron-transfer routes. Each of two predicted intramolecular electron-transfer pathways within the complex may be biologically relevant.

2.3.3 Number of transferred electrons and its significance for the electron transfer mechanism

The earliest potentiometric titration studies on adrenodoxin revealed that the number of electrons transferred per mole of Adx, generally known as one-electron carrier protein, is two [Kimura & Suzuki, 1967]. This result is also supported by anaerobic titration with NADPH in the presence of AR [Kimura & Suzuki, 1965]. The present study supports this observation. The observed Nernst slopes of ~30 mV for Adx(WT), Adx(1-108), and $Ru(bpy)_2(mbpy)$-Adx(1-108) indicate that the dye-associated photoreduction of Adx is accompanied by a transfer of two

electrons from safranin T (Figure 2.2.7.1) to each of the ferredoxins. Thus, the transfer of the first electron to Adx might trigger the acceptance of the second electron. Consequently, the question arises where the second electron is bound or how it is consumed, while the first electron is used for the iron-sulfur cluster reduction. Indeed, a spin quantification indicates that just one of the two iron atoms is in the Fe^{2+}-state as detected by EPR (Figure 2.2.11.1, trace a). Moreover, the Nernst slope of 66 mV for $P450_{cam}$ as for a typical one-electron acceptor protein and a correct application of the photoreduction method, indicate a transfer of one electron only, as expected. At present, the answer to the question of the second electron, which is transferred to Adx needs further investigation, but the following suggestion may be reasonable.

Although Adx(4-108) was monomeric in the crystal structure [Müller et al., 1998] dimeric Adx has been identified by dynamic light scattering [Pikuleva et al., 2000]. From the cross-linking studies on bovine Adx(WT) and Adx(4-108) it was clarified that dimers exist only in the oxidized state, whereas the proteins were monomeric in the reduced state [Beilke et al., 2002]. That was also confirmed at low protein concentrations, when the reduced state was analyzed by native gel electrophoresis and gel filtration experiments [Beilke et al., 2002]. *Tsubaki et al.* [Tsubaki et al., 1989] have shown that reduced Adx can form a 1:1 complex with reduced $P450_{scc}$, suggesting that dimer formation of Adx [Pikuleva et al., 2000] during electron transfer (during turnover conditions, i.e. during side-chain cleavage activity of $P450_{scc}$) is unlikely *in vivo* [Takeuchi et al., 2001]. Thus, possible oxidized Adx dimer can inhibit the $P450_{scc}$ activity by binding to the cytochrome with twice the affinity of the reduced monomeric protein, and as it does oxidized Adx [Lambeth & Pember, 1983; Tuckey et al., 2001], and hence, indicating that the "shuttle" model is active in the electron transfer only. Nevertheless, *Beilke et al.* [Beilke et al., 2002] have proposed a mechanism of electron transfer *via* Adx dimers that supplements the "shuttle" model suggested by *Lambeth et al.* [Lambeth et al., 1982]. From the physiological point of view, as pointed out by *Beilke et al.* [Beilke et al., 2002], the dimers might have functional significance and could also explain present results.

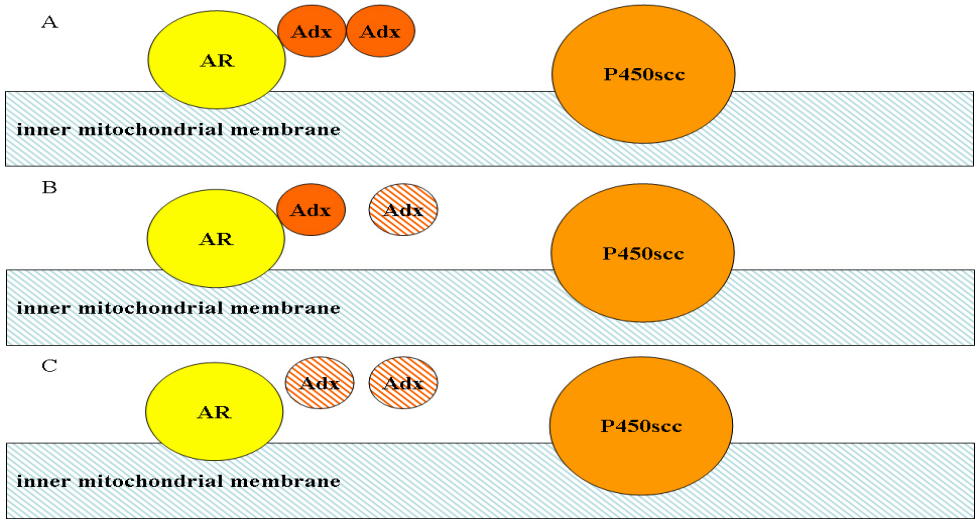

Figure 2.3.3.1 Schematic representation of the mechanism of action of an Adx dimer, according to *Beilke et al.* [Beilke et al., 2002]. A. An oxidized dimer of Adx binds to AR. NADPH (it is not shown) supplies two electrons to AR. B. One electron is transferred to the “distal” Adx molecule not interacting with AR. Its reduction leads to dissociation of the ferredoxin dimer. C. Dissociation of the Adx dimer allows reduction of the second Adx molecule still bound to AR. After the last Adx is reduced, it dissociates from AR. As next step, two reduced Adx molecules can bind to $P450_{scc}$ to supply the electrons to the heme protein. Oxidized and reduced Adx molecules are drawn as closed orange circle and striped orange circle, respectively.

The Nernst slope of each of the investigated adrenodoxins would suggest that each of the two electrons was used for one single reduction step of each Adx molecule in a dimer, however, in a sequential manner. Initially, the first reduction of one of the two adrenodoxin molecules in the dimer would initiate a cascade of the following processes: (i) conformational change in the first reduced molecule leading to (ii) dissociation of the dimer and (iii) finally, as a consequence of (i) and (ii), triggering the reduction of the second oxidized Adx presumably by facilitating the access of the reducing species to the site relevant for the electron jump (Figure 2.3.3.1). Thus, the targets here are two redox centers of two adrenodoxin molecules in one dimer.

There is no crystal structure of a cross-linked Adx dimer that would provide some information about the dimerization process of Adx. Two known crystal structures of bovine Adx [Müller et al., 1998; Pikuleva et al., 2001] describe two possible so-called Adx “dimers”[25] (Figure 2.3.3.2). It is more likely that the C-terminal tail of Adx(WT) plays a role in dimerization of Adx [Pikuleva et al., 2001] (Figure 2.3.3.2.A), but the possibility of the existence of a truncated dimer is not excluded [Beilke et al., 2002].

[25] Here and further in the discussion of Adx dimerization based on the crystal structures of truncated and full-length protein, the word dimer will be printed in inverted commas, since it is not proven that Adx form dimers.

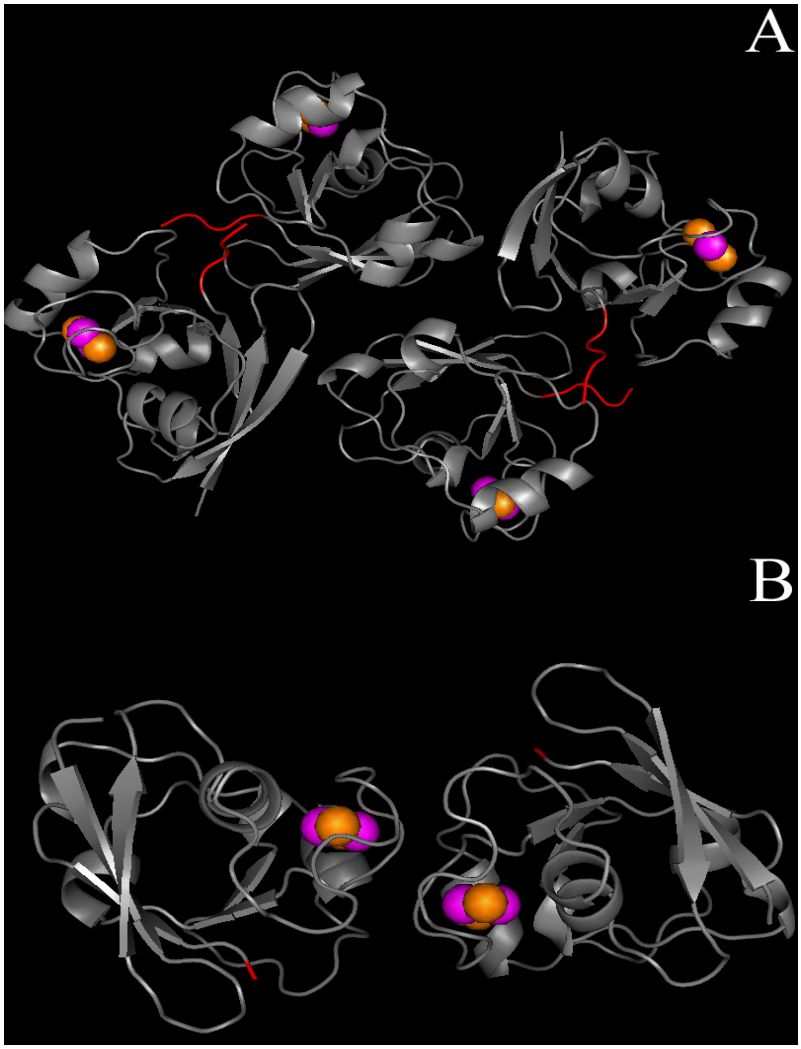

Figure 2.3.3.2 “Dimers”of Adx (grey). A. Full-length Adx [Pikuleva et al., 2001]. B. Adx(4-108) [Müller et al., 1998]. The [2Fe-2S] cluster is in sphere view with the iron atoms in magenta and sulfurs in orange. The C-terminal tail (residues starting from Pro108) of Adx is shown in red. Picture generated using PyMOL.

If one still assumes that Adx forms dimer then it should be a homodimer, i.e. a dimer between two oxidized proteins [Beilke et al., 2002]. Homodimers are the simplest example of the non-covalent self-assembly of proteins. Their subunit interfaces, defined as the regions of the protein surface that are involved in subunit contacts, display geometric and chemical properties that give the assembly its stability and specificity [Bahadur et al., 2003]. The size of interchain contacts in protein crystals, usually measured by ASA, can be exploited to discriminate functional subunit-subunit interface against unspecific contacts that are artefacts of the crystal packing [Janin 1997; Janin & Rodier, 1995]. Crystal packing generally involves interfaces that are much smaller and less hydrophobic than in protein-protein complexes or oligomers [Valdar & Thornton, 2001; Janin 1995].

In homodimer, twofold symmetry implies that each component contributes equally to *B*, which is not necessarily the case in a heterodimer [Bahadur et al., 2003]. The average *B*/2 values for 1CJE, 1AYF, and 2BT6 were 533 Å (chainA-chainB interface) and 504 Å (chainC-chainD

interface); 372 Å (chainA-chainB interface); and 328 Å (chainA-chainB interface), respectively. Homodimeric proteins interfaces bury 16% of the subunit surface on average, with variation from 3% to 44%, which corresponds to *B*/2 from 500 Å to 7,000 Å [Bahadur et al., 2003]. Although small proteins obviously cannot form very large interfaces, the correlation with the size is mediocre ($R^2 = 0.34$) [Bahadur et al., 2003]. Thus, Adx in three structures is more likely monomeric than dimeric. However, the distinction between monomeric and oligomeric state, in general, cannot be made with more than 85-90% confidence, while there is no well-proved biochemical information, confirming the fact that dimer of a protein exists in the solution [Valdar & Thornton. 2001; Ponstingl et al., 2000]. Thus, additional biochemical and crystallographic studies will be required to check the dimerization of Adx.

Transport of two electrons – other idea. The difference spectra of chemically reduced and photoreduced Adx show some differences in the visible range (Figure 2.2.10.1.B). These are probably due to the fact that dithionite can supply two electrons [Lambeth & Palmer, 1973] and ruthenium complex only one electron that will be used per mole of the protein. The latter is true if one uses sacrificial electron donor EDTA to avoid back electron transport[26]. This was also the main idea of this thesis that the iron-sulfur cluster stays reduced after illumination of the $Ru(bpy)_2(mbpy)$-Adx(1-108) sample. However, doing so EDTA will provide under continued irradiation of the $Ru(bpy)_2(mbpy)$-Adx(1-108) complex, the transport of another (second) electron from the same ruthenium moiety within the complex with already reduced Adx, but now to a neighboring $Ru(bpy)_2(mbpy)$-Adx(1-108) complex in which the protein is oxidized. The intermolecular electron transfer will take place. Thus, the ruthenium moiety can quasi supply two electrons, which will be used only by two different Adx molecules.

The chemically reduced [2Fe-2S] cluster shows the difference spectrum as in Figure 2.2.10.1.B (black spectrum) with two minima at 414 nm and 450 nm. These minima are also present in the difference spectrum of the light-reduced Adx (Figure 2.2.10.1.B, blue spectrum), but with a slight shift to longer wavelengths due to the spectral contribution of the ruthenium complex. The shapes of these two difference spectra discriminate in the wavelength range between 490 nm and 650 nm. But, it was shown that after addition of dithionite to the sample of $Ru(bpy)_2(mbpy)$-Adx(1-108) (data not shown), its difference spectrum became similar to that of

[26]EDTA has been used a sacrificial electron donor, that reacts irreversibly with Ru^{3+} to form Ru^{2+} The rate of EDTA oxidation is $k_Q = 1.1 \times 10^8$ $M^{-1}s^{-1}$ [Keller et al., 1980]. The usage of 100 mM EDTA ensures that all Ru^{3+} formed during illumination is instantaneously reduced to Ru^{2+}, thus minimizing the Fe^{2+} / Ru^{3+} back transfer, and that the EDTA concentration can be assumed as constant during the experiment.

the unmodified protein, which was chemically reduced. Moreover, because the absolute extent of the reduction is small in the photoreduction experiment, the spectral changes of Adx and of the ruthenium complex might compensate against each other. This would, however, implicate that small changes of the ruthenium complex occur under illumination, which were indeed also observed when the ruthenium complex alone was illuminated. At present, the reason for the observed spectral differences is not clear, but it may help to answer the question about the second electron that is transferred to Adx during reduction.

In spite of the spectral differences and may be differences in the reduction mechanism, the EPR spectra of the (photo)reduced [2Fe-2S] cluster are almost identical. The EPR spectrum of the chemically reduced Adx samples shows two species ($g_{\|}$ = 2.024(2), $g\perp$ = 1.938(2) and $g_{\|}$ = 2.012(2), $g\perp$ = 1.942(2)), which might reflect a mixture of each of the reduced Adx molecules of the original dimer or a mixture of subconformers whose population is dependent on pH, solvent conditions, and freezing procedure, which have been also described elsewhere [Mukai et al., 1973]. The ruthenium complex-coupled Adx does not possess specific new *g*-values, but shows only changed population equilibrium of the two species, indicating that the iron-sulfur cluster is not affected just by the labeling (Figure 2.2.11.1, trace d).

In summary, the photoreduction of Adx(1-108) has been successfully established, which encourages to further develop this approach to study electron transfer to $P450_{scc}$ *via* the $Ru(bpy)_2(mbpy)$-Adx(1-108) complex. This might help to reveal the fundamental mechanism of electron transfer in the mitochondrial monooxygenase system.